DISCLAIMER

This contractor document was prepared for the U.S. Department of Energy (DOE), but has not undergone programmatic, policy, or publication review, and is provided for information only. The document provides preliminary information that may change based on new information to be used specifically for Total System Performance Assessment analyses. The document is a preliminary lower-level contractor document and is not intended for publication or wide distribution.

Although this document has undergone technical reviews at the contractor organization, it has not undergone a DOE policy review. Therefore, the views and opinions of authors expressed may not state or reflect those of the DOE. However, in the interest of the rapid transfer of information, we are providing this document for your information per your request.

OFFICE OF CIVILIAN RADIOACTIVE WASTE MANAGEMENT
ANALYSIS/MODEL COVER SHEET

Complete Only Applicable Items

1. QA: QA

2. ☐ Analysis — Check all that apply		3. ☒ Model — Check all that apply	
Type of Analysis	☐ Engineering ☐ Performance Assessment ☐ Scientific	Type of Model	☒ Conceptual Model ☒ Abstraction Model ☒ Mathematical Model ☐ System Model ☒ Process Model
Intended Use of Analysis	☐ Input to Calculation ☐ Input to Another Analysis or Model ☐ Input to Technical Document ☐ Input to Other Technical Products	Intended Use of Model	☐ Input to Calculation ☒ Input to Another Model or Analysis ☒ Input to Technical Document ☒ Input to Other Technical Products
Describe use:		Describe use:	Model to be used in the simulation of radionuclide migration in the saturated zone.

4. Title:

Saturated Zone Transport Methodology and Transport Component Integration

5. Document Identifier (including Rev. No. and Change No., if applicable):

MDL-NBS-HS-000010, Rev. 00

6. Total Attachments:	7. Attachment Numbers - No. of Pages in Each:
1	I: 6

	Printed Name	Signature	Date
8. Originator	Bruce Robinson		7-10-00
9. Checker	Chunhong Li		7/10/00
10. Lead/Supervisor	Al Eddebbarh		7/10/00
11. Responsible Manager	Paul Dixon	Frank Perry for Paul Dixon	7/10/00

12. Remarks:

INITIAL ISSUE

INFORMATION COPY

LAS VEGAS DOCUMENT CONTROL

OFFICE OF CIVILIAN RADIOACTIVE WASTE MANAGEMENT
ANALYSIS/MODEL REVISION RECORD

Complete Only Applicable Items

2. Analysis or Model Title:

Saturated Zone Transport Methodology and Transport Component Integration

3. Document Identifier (including Rev. No. and Change No., if applicable):

MDL-NBS-HS-000010, Rev 00

4. Revision/Change No.	5. Description of Revision/Change
00	Initial issue

CONTENTS

INTENTIONALLY LEFT BLANK

FIGURES

TABLES

INTENTIONALLY LEFT BLANK

ACRONYMS

AMR	Analysis and Modeling Report
CM	Configuration management
CRWMS M&O	Civilian Radioactive Waste Management System Management and Operating Contractor
OCRWM	Office of Civilian Radioactive Waste Management
PA	Performance Assessment
PMR	Process Model Report
QA	Quality assurance
RTTF	Residence time transfer function
SAN	Software Activity Number
SR	Site Recommendation
STN	Software Tracking Number
SZ	Saturated zone
TSPA	Total Systems Performance Assessment
TSPA-SR	Total Systems Performance Assessment-Site Recommendation
TSPA-VA	Total Systems Performance Assessment-Viability Assessment
UZ	Unsaturated zone
V	Version
VA	Viability Assessment

INTENTIONALLY LEFT BLANK

1. PURPOSE

The purpose of the transport methodology and component analysis is to provide the numerical methods for simulating radionuclide transport and model setup for transport in the saturated zone (SZ) site-scale model. The intended use of this model is to simulate transport in saturated porous rock under natural or forced gradient flow conditions. The particle-tracking method of simulating radionuclide transport is incorporated into the FEHM Version (V) 2.10 [Software Tracking Number (STN): 10086-2.10-00] computer code, which is a three-dimensional, finite element flow and transport code. The resulting changes in the FEHM code are to be submitted to the software configuration management (CM) system.

This Analysis/Model Report (AMR) establishes the requirements and elements of the design of a methodology for calculating radionuclide transport in the saturated zone at Yucca Mountain in support of Total Systems Performance Assessment (TSPA). Concurrently, process-level flow model calculations are being carried out in an AMR for the saturated zone (CRWMS M&O 2000a) using FEHM. In previous TSPA analyses, a simplified system of one-dimensional streamtubes was envisioned to characterize the radionuclide plume. Parameters such as dilution factor and effective porosity were used to model radionuclide transport within each streamtube, with the composite concentration then determined by superimposing the solutions from the individual streamtubes. This analysis had severe limitations, including the lack of physical basis for the streamtubes, the difficulty in superimposing the solutions in a reasonable fashion, and the lack of process-level detail in both the flow patterns and the transport processes.

To improve on the work performed so far for the saturated-zone flow and transport modeling, concerted effort has been made in two areas. First, the characterization of the hydrogeology and description of the flow system in the aquifer beneath Yucca Mountain has been updated and improved (CRWMS M&O 2000a). Second, the methodology for computing transport of radionuclides within the saturated zone has been revised to capture a variety of different processes with accuracy. The subject of this AMR is the methodology for radionuclide transport. In this document, we outline the requirements of a radionuclide transport mathematical and computational model that satisfies the requirements of the project, which is to produce scientifically defensible transport predictions. In the process, we address issues raised by reviewers of both the saturated-zone flow and transport modeling effort and the TSPA Viability Assessment (VA) abstracted model for radionuclide transport in the saturated zone. We then develop the numerical techniques required to implement the method and perform a series of test cases for the model.

Several code validation cases are presented to demonstrate that the code agrees with accepted analytical solutions. These tests are not models of the Yucca Mountain saturated zone, but merely demonstrate that the mathematical principles and assumptions are properly implemented

in the code. Therefore, the values of hydrologic parameters used for the testing are not based on Yucca Mountain values, but are merely selected for convenience. The test cases demonstrate that when the particle-tracking model is employed by those simulating transport in the saturated zone, the code is functioning properly.

This work is being performed in accordance with the planning outlined in CRWMS M&O (1999a).

2. QUALITY ASSURANCE

The activities documented in this AMR were evaluated in accordance with QAP-2-0, Rev 5, *Conduct of Activities*, and were determined to be subject to the requirements of the U.S. DOE Office of Civilian Radioactive Waste Management (OCRWM) *Quality Assurance Requirements and Description* (QARD) (DOE 2000). This evaluation is documented in CRWMS M&O (1999b-d) and Wemheuer (1999, Activity Evaluation for Work Package 1401213SM1). This AMR has been prepared in accordance with procedure AP-3.10Q, *Analyses and Models*.

The activities documented in this AMR do not involve the storage, maintenance, retrieval, or transmittal of quality-affecting data or information using electronic media and do not require the implementation of process controls in accordance with AP-SV.1Q, *Control of the Electronic Management of Data*.

INTENTIONALLY LEFT BLANK

3. COMPUTER SOFTWARE AND MODEL USAGE

The computer software code used as the basis to perform/model the saturated-zone particle tracking in this AMR is FEHM V2.0 (STN: 10031-2.00-00) for a SUN Ultra Sparc, Unix platform. However, this version of the code was not used in any calculations but only as the starting point for code development. A revised version of the code that includes the particle-tracking algorithm described in this AMR is currently being qualified under AP-SI.1Q, *Software Management*, as FEHM V2.10 (STN: 10086-2.10-00). Version 2.10 is the version used for all calculations performed in this AMR; therefore, the software is currently unqualified and all results require confirmation. FEHM V2.10 was used in accordance with Section 5.11 of AP-SI.1Q.

The input and output files for these analyses are found in DTN: LA9912BR12213S.001.

The software routine 3DADE is used to solve analytical solutions to validate the particle-tracking model. This single-use routine is identified in Table 1 and documented in Attachment I.

Table 1. Computer Software and Routines

Software Name	Version	Software Tracking Number (STN)	Computer Platform
FEHM	2.10	10086-2.10-00	SUN with UNIX OS, FORTRAN
Software Routine		**Documentation**	
3DADE	Rev 00	Attachment I	SUN with UNIX OS, FORTRAN

In addition, the graphics software package FORTNER PLOT SUN Workstations V1.3 was used in this analysis and documentation for plotting graphs. It was not used in any quality-affecting work.

INTENTIONALLY LEFT BLANK

4. INPUTS

4.1 DATA AND PARAMETERS

There are no site-specific data or parameters used in this AMR. All simulations are carried out with appropriate values of hydrologic and transport parameters, that is, values similar to those to be used in the saturated-zone flow and transport modeling activities. However, the numerical simulations performed in this AMR do not require referenceable parameter values.

4.2 CRITERIA

This AMR complies with the DOE interim guidance (Dyer 1999). Subparts of the interim guidance that apply to this analysis or modeling activity are those pertaining to the characterization of the Yucca Mountain site (Subpart B, Section 15), the compilation of information regarding hydrology of the site in support of the License Application (Subpart B, Section 21(c)(1)(ii)), and the definition of hydrologic parameters and conceptual models used in performance assessment (Subpart E, Section 114(a)).

4.3 CODES AND STANDARDS

No specific formally established codes or standards have been identified as applying to this modeling activity.

INTENTIONALLY LEFT BLANK

5. ASSUMPTIONS

1) *Particle tracking is a numerical technique that is acceptable for simulating the transport of radionuclides in the saturated zone at Yucca Mountain (assumption used throughout document).* Particle-tracking techniques have a long history of use in such applications (e.g., Pollock 1988; Tompson and Gelhar 1990; Wen and Gomez-Hernandez 1996), thereby justifying this assumption. This assumption does not require verification.

2) *The anisotropic dispersion coefficient tensor developed in this AMR is suitable for characterizing dispersion via the random walk particle-tracking method (used in Section 6.1).* Random-walk techniques have been derived rigorously in the past (e.g., Tompson et al. 1987; Tompson and Gelhar 1990) and have been accepted by the hydrologic community for simulating dispersion. The use of a dispersion coefficient tensor is an appropriate simplification for characterizing dispersion, as evidenced by its use as the starting point in virtually all numerical flow and transport codes. The particular form derived in this AMR reflects the need to account for different dispersivity values in the directions normal to the local flow direction, as shown in field studies discussed by Gelhar (1997, p. 164, Figure 8). This assumption does not require verification.

3) *Matrix diffusion can be characterized using an abstracted model of uniform flow and transport in equally spaced, parallel fractures (used in Section 6.2).* Because the particle-tracking model is intended to be used in large-scale simulations, the size of a computational grid block is likely to be much greater than the typical fracture spacing. In such circumstances, the use of an effective spacing to capture the transport behavior is reasonable. Although the constant-spacing assumption is not literally true, it can be justified on the basis of the impossibility of acquiring the data needed to completely characterize the location and flow rate of every fracture in the saturated zone. In numerical modeling studies, such uncertainties are commonly addressed through the use of simpler conceptual models such as this one, combined with sensitivity analyses to assess the importance of the uncertain parameters to the final model result. Therefore, it is recommended that when this model is used, that a broad range of fracture spacings be used and the influence on the final results be quantified. This assumption does not require verification.

INTENTIONALLY LEFT BLANK

6. ANALYSIS/MODEL

The model documented in this AMR does not provide estimates of any of the factors included in the Post-Closure Safety Case and was deemed to be of Level 3 importance pursuant to AP-3.10Q.

In this section we outline the requirements of the radionuclide transport model as the first step toward developing the computational and mathematical models needed in Performance Assessment (PA) calculations.

1. The transport model predictions must be based on a three-dimensional process-level flow model.

The TSPA-VA streamtube model (DOE 1998, p. 3-139, Figure 3-68) was an abstraction with little physical basis. In the upcoming TSPA analysis, we will formulate calculations directly using a process-level flow model. Three-dimensional effects are deemed to be important, so the transport of radionuclides should be based directly on the best available model at the time the calculations must be completed. This improvement will also have the advantage of compatibility with the unsaturated-zone flow and transport model in terms of its complexity and lack of significant simplifications when implemented in the TSPA Site Recommendation (SR) calculations.

In addition to consistency, it is advantageous to base transport predictions on the same models used in flow-model sensitivity studies. As outlined in the Work Package Planning Summary (CRWMS M&O 1999d) for the Saturated Zone Process Model Report (PMR), sensitivity to hydrogeologic framework uncertainties, climate change, and hydrologic parameter uncertainty are all being carried out. By predicting transport behavior for all of these scenarios and assessing the significance of the uncertainties, the flow and radionuclide transport predictions included in the TSPA calculations will be a subset of a larger number of flow and transport simulations carried out by the flow-model development team. Finally, transport of natural environmental tracers and dissolved species will be performed as part of the three-dimensional model development. Therefore, radionuclide transport predictions based on the same flow and transport model will lend credibility to the predictions.

The transport model must be able to handle extremes of the advective-dispersive transport that include a wide range of dispersivity values. Without evidence to the contrary, dispersivity values transverse to the flow direction should be assumed to be low to avoid overestimating the amount of radionuclide dilution caused by transverse dispersion. For example, transverse dispersivity values measured at field sites such as the Borden, Cape Cod, and Condie aquifers, were on the order of millimeters to centimeters in the vertical direction (e.g., Gelhar 1997, Figure 8, p. 164). Theoretical studies (CRWMS M&O 2000b) have also shown that small values of transverse vertical dispersivity are appropriate. Capturing this low level of dispersion transverse to the mean trajectory of a solute plume is extremely difficult using typical finite-element or finite-volume transport models unless extraordinarily fine grid discretization is employed. Furthermore, the final few kilometers (km) of travel to a 20- or 25-km compliance point will be through alluvial deposits, for which the scientific community has determined that low transverse

dispersivity is likely (Gelhar 1997, p. 164, Figure 8). Therefore, the model must be able to handle cases of low transverse dispersivity, including a value of 0, throughout the entire travel path or larger dispersivity in the fractured volcanic rocks transitioning abruptly to low dispersivity in the alluvium.

The method for introducing the radionuclide source term into the model must be flexible enough to handle both small and large source regions at the water table. In the TSPA-VA abstracted transport model for the saturated zone (DOE 1998), large source regions were assumed over which radionuclides were introduced to the saturated-zone model. Spreading of radionuclide mass (computed from the unsaturated-zone flow and transport model) over large areas would only be valid if the source at the repository is due to many waste packages leaking simultaneously and if there is sufficient transverse dispersion within the unsaturated zone to smear the source within the percolating unsaturated-zone fluid. Although smearing the radionuclide mass may be a good assumption under some circumstances, the case of releases from a small number of waste packages clearly cannot be handled with such a model. For example, in the first 10,000 years for the TSPA-VA base-case model, only a few tens of waste packages had failed. Taking radionuclide mass releases from this system and smearing them over large areas introduces large, artificial dilution factors at the unsaturated-zone–saturated-zone (UZ-SZ) interface. It is important to point out that this modeling decision was probably counteracted by an overly conservative dilution factor for transport within the saturated zone, especially for the case of transport of small individual "microplumes" in the aquifer. Instead of counteracting a nonconservative assumption with a conservative one and hoping that the final answer is correct, the new transport model must be able to handle small source regions.

2. *It may be necessary to compute the transport of plumes that have smaller dimensions than the grid block size of the flow model.*

The need to simulate "microplume" transport was alluded to above. If these plumes have characteristic dimensions that are of the same order or smaller than the grid block size of the flow simulation, then finite-element simulations of transport cannot capture the details of radionuclide spreading. Numerical dispersion effects arising from such an approach can easily be misinterpreted as dilution. A numerical method that retains the accuracy of the local concentration for small plumes is required. In this model we use the method of Pollock (1988) to estimate the velocity field at the sub-grid block level through velocity interpolation. This method is commonly accepted for particle-tracking algorithms.

3. *The transport model must capture the important physicochemical processes known or suspected to occur in fractured porous rock.*

In the TSPA-VA calculations, the effective porosity was used as an uncertain parameter that was assumed to capture the intricacies of transport through fractured rock. The distribution of this uncertain parameter was set using the results of the Expert Elicitation (CRWMS M&O 1998). A side effect of this approach was that sorption coefficients had to be adjusted along with the effective porosity in an attempt to achieve a conservative result, that is, a result that, if anything, yields a higher dose than would have been obtained with a more rigorous formulation. This approach needs to be improved in the new transport model formulation. Reimus et al. (1999) have shown that the behavior of the C-wells reactive tracer test can be explained using a dual-

porosity transport model that includes matrix diffusion and sorption on the matrix rock. Previously, Robinson (1994) proposed that a matrix-diffusion model should be used to model transport of radionuclides in the saturated zone and demonstrated that the C-wells experiments (not yet carried out at the time of Robinson's paper) be used to validate this concept. The proposed model was based on numerous theoretical and experimental studies of transport in fractured rock. The fact that the test results are consistent with the matrix-diffusion model implies that the radionuclide transport model, to be consistent with the results of the field experiment, must have a dual-porosity transport formulation. We, therefore, develop a dual-porosity transport model for characterizing transport in fractured tuff. Sorption coefficients are applied to the matrix domain and come into play only if significant diffusion into the matrix pores occurs as radionuclides travel through the system. This transport model is much more physically based, is consistent with field studies carried out in a variety of fractured rocks, including at Yucca Mountain and the Nevada Test Site, and thus is far more defensible than the approach taken in TSPA-VA. To implement the dual porosity transport model, a particle-tracking approach is taken in which aqueous species are modeled as discrete particles. An additional benefit of this approach is that particle tracking is also being used in the unsaturated-zone transport model.

4. *It must be possible to abstract the results of the process-level transport model for use in TSPA-SR calculations.*

The main purpose of the radionuclide transport model is to predict the concentrations within the aquifer so that pumping-well or other water-use scenarios can be constructed. Concentrations are then converted to dose using biosphere models. One "end-product" of the saturated-zone radionuclide transport model is, therefore, a spatial and temporal distribution of radionuclides within the aquifer. In TSPA-VA (DOE 1998, p. 3-142, Figure 3-69), the concentration within the saturated zone was computed as a unit breakthrough curve, which is defined as the response to a steady-state mass flux input at the footprint of the repository at the water table. These breakthrough curves were converted to actual concentrations at the compliance point through numerical convolution using the source term computed from the unsaturated-zone flow and transport model. Because a similar abstraction is being employed in TSPA-SR, breakthrough curves at the compliance point will again be a required output of the saturated-zone model. These breakthrough curves do not need to consider radioactive decay because that process is considered during the numerical convolution step. In addition to providing distributions of arrival times, another desirable feature of the model is to allow for the calculation of *in situ* concentrations of radionuclide concentration at specified locations in the model.

To implement a model with assumptions just listed, a particle-tracking method was used to simulate solute transport. Particle-tracking methods provide an efficient numerical algorithm for modeling large-scale transport of solutes in heterogeneous porous media (Tompson and Gelhar 1990). By contrast, continuum approaches involving finite-difference or finite-element solution methods generally suffer from numerical dispersion, primarily because of the large grid blocks required to model large-scale systems. Furthermore, using particle tracking, plumes can be simulated at scales smaller than the grid block size, and source regions (zones in which particles are initially placed) can be smaller than the grid spacing. Therefore, the primary numerical requirements listed in Section 5 are satisfied by using a particle-tracking model approach.

In this section the particle-tracking technique is briefly summarized, and in subsequent sections a detailed description of the mathematical method is provided. Transport is decomposed into three interrelated components: advective, dispersive, and physicochemical. For the advective component, the particle-tracking method developed here is based on the Lagrangian point of view, in which particles move with the prevailing flow velocity. To do this, the hydraulic heads computed at each node of the computational mesh in the flow solution are used, along with Darcy's law, to compute the velocities at the finite volume cell faces surrounding each node. Trajectories are computed for one particle at a time. The advective component of the solute transport is computed using the method of Pollock (1988). In this method, a semianalytical solution to the particle tracks is obtained by interpolating the flow velocities linearly within each computational cell, permitting the flow lines to be computed in an efficient manner. The exit time of a particle entering a computational cell is determined from the semianalytical solution. Then, to incorporate dispersion, the model takes small increments of time during the advective transport steps to calculate the displacement of the particle due to dispersion. The dispersive component of the transport is calculated using the random-walk method (Tompson and Gelhar 1990). This approach is based on the analogy between the mass transport equation and the Fokker-Plank equation of statistical physics (Van Kampen 1981). The dispersive displacement of each particle is computed using uniform random numbers, based on the dispersivity tensor and the porous flow velocity field at the particle location. In this model, the proper terms in the random-walk algorithm are derived from an anisotropic version of the dispersion coefficient tensor defined by Burnett and Frind (1987). Finally, the sorption and diffusion processes are captured using a matrix-diffusion submodel, which delays particles in accordance with a semianalytical solution that includes sorption and diffusion into the rock matrix away from the flowing fractures. Linear equilibrium sorption and diffusion from equally spaced fractures into a stagnant matrix fluid are assumed.

6.1 ADVECTIVE-DISPERSIVE TRANSPORT

The fundamental mass transport equation for transport of a nonreactive, dilute species in a saturated porous medium (with no sources or sinks) has the form (e.g., Bear 1988, p. 617, Equation 10.5.2):

$$\frac{\partial C}{\partial t} + \nabla \cdot (\bar{v} C) - \nabla \cdot (D \nabla C) = 0, \qquad \text{(Eq. 1)}$$

where

C denotes the solute concentration in units of moles per liter
t is time
$\bar{v}$ designates the solute average pore-water velocity vector
D denotes the dispersion tensor.

This equation serves as the starting point for all subsequent development below.

For an isotropic medium, the dispersion has the form (Bear 1988, p. 615):

$$D_{ij} = \alpha_T v \delta_{ij} + (\alpha_L - \alpha_T)\frac{v_i v_j}{v} + D_0 \delta_{ij}, \qquad \text{(Eq. 2)}$$

where

α_L and α_T denote the longitudinal and transverse dispersivities, respectively
D_0 represents the molecular diffusion constant
i and j are indices representing the coordinate directions
δ_{ij} is the Kronecker delta function
$v = |\vec{v}|$ is the magnitude of the velocity vector.

Defining the three Cartesian coordinate axes as 1, 2, and 3, the dispersion tensor given in Equation 2 can be written in matrix form as

$$D - D_0 I = \begin{pmatrix} \alpha_T v + (\alpha_L - \alpha_T)\frac{v_1^2}{v} & (\alpha_L - \alpha_T)\frac{v_1 v_2}{v} & (\alpha_L - \alpha_T)\frac{v_1 v_3}{v} \\ (\alpha_L - \alpha_T)\frac{v_2 v_1}{v} & \alpha_T v + (\alpha_L - \alpha_T)\frac{v_2^2}{v} & (\alpha_L - \alpha_T)\frac{v_2 v_3}{v} \\ (\alpha_L - \alpha_T)\frac{v_3 v_1}{v} & (\alpha_L - \alpha_T)\frac{v_3 v_2}{v} & \alpha_T v + (\alpha_L - \alpha_T)\frac{v_3^2}{v} \end{pmatrix}. \qquad \text{(Eq. 3)}$$

where I is the identity matrix. In an anisotropic system, the expression for the dispersion tensor is more complex, involving as many as 36 independent parameters to characterize (Bear 1988, p. 611). Burnett and Frind (1987) proposed a simplified form that we have adopted in the particle-tracking algorithm. This representation of the dispersion tensor contains three parameters: longitudinal (α_L), transverse horizontal (α_T^H), and transverse vertical (α_T^V) dispersivities. This formulation was chosen because of its relative simplicity and correspondence to the primary terms normally estimated in field studies. Particle-tracking models based on the more common dispersion coefficient tensor of Equations 2 and 3 do not allow the transverse dispersivities to be set to different values in the horizontal and vertical directions and, hence, is inadequate for the present purposes. For the anisotropic model, the dispersion tensor has the form:

$$D - D_0 I = \begin{pmatrix} \alpha_L \frac{v_1^2}{v} + \alpha_T^H \frac{v_2^2}{v} + \alpha_T^V \frac{v_3^2}{v} & (\alpha_L - \alpha_T^H)\frac{v_1 v_2}{v} & (\alpha_L - \alpha_T^V)\frac{v_1 v_3}{v} \\ (\alpha_L - \alpha_T^H)\frac{v_2 v_1}{v} & \alpha_T^H \frac{v_1^2}{v} + \alpha_L \frac{v_2^2}{v} + \alpha_T^V \frac{v_3^2}{v} & (\alpha_L - \alpha_T^V)\frac{v_2 v_3}{v} \\ (\alpha_L - \alpha_T^V)\frac{v_3 v_1}{v} & (\alpha_L - \alpha_T^V)\frac{v_3 v_2}{v} & \alpha_T^V \frac{\left(v_1^2 + v_2^2\right)}{v} + \alpha_L \frac{v_3^2}{v} \end{pmatrix}. \qquad \text{(Eq. 4)}$$

We have determined that, in particle-tracking methods, incorporation of the off-diagonal terms of the dispersion tensor is important for obtaining the proper behavior for dispersion parallel and perpendicular to the direction of flow when flow is not parallel to any of the coordinate axes, as in a heterogeneous flow field, for example. When the off-diagonal terms are omitted, particle-

plume spreading exhibits an orientation effect along the coordinate axes even when the flow is not oriented with the axes. To prevent this non-physical behavior, all of the terms in Equation 4 are retained in the model development below.

Given a steady-state velocity field generated, for example, for an arbitrary permeability field, a random walk is superimposed on the flow field to describe dispersion and molecular diffusion. The general approach used in particle tracking is to replace the partial differential equation for the solute concentration C, generally expressed by Equation 1, with random-walk displacements defined in differential form by the Langevin equation (Gardiner 1997, p. 80):

$$dx = A(x,t)dt + B(x,t)dW(t), \qquad \text{(Eq. 5)}$$

for position vector $x(t)$. The matrix A represents the deterministic background displacement determined by $\vec{v}$ and, in addition, contains contributions from the dispersion tensor. The displacement matrix B refers to a stochastic random-walk process that incorporates molecular diffusion and dispersion. The differential $dW(t)$ represents a Wiener process describing Brownian motion with the properties:

$$< dW > = 0, \qquad \text{(Eq. 6)}$$

and

$$< dW(t)dW(t) > = Idt, \qquad \text{(Eq. 7)}$$

where the angular brackets represent the ensemble mean.

The equivalent Fokker-Plank equation corresponding to the Langevin equation (Equation 5) for the conditional probability $P(x,t|x_0,t_0)$ is given by (Gardiner 1997, p. 97):

$$\frac{\partial P}{\partial t} = -\nabla \cdot [A(x,t)P] + \nabla : \nabla \left[\frac{1}{2} B\tilde{B}P \right], \qquad \text{(Eq. 8)}$$

where $\tilde{B}$ represents the transpose matrix. The Fokker-Plank equation may be written in the form of the transport equation by rearranging Equation 8 to obtain

$$\frac{\partial P}{\partial t} = -\nabla \cdot \left[\left(A(x,t) - \frac{1}{2} \nabla \cdot B\tilde{B} \right) P \right] + \nabla \cdot \left[\frac{1}{2} B\tilde{B} \nabla P \right]. \qquad \text{(Eq. 9)}$$

Comparing this modified Fokker-Plank equation with the continuum-based transport equation given in Equation 1 yields the identifications

$$P(x,t \mid x_0,t_0) = \frac{N_A}{N} C(x,t), \qquad \text{(Eq. 10)}$$

where N represents the number of particles and N_A denotes Avogadro's number,

$$A(x,t) = \vec{v} + \nabla \cdot D, \qquad \text{(Eq. 11)}$$

and

$$\frac{1}{2}B\tilde{B} = D. \qquad \text{(Eq. 12)}$$

Therefore, it is necessary to obtain the displacement matrix B based on the dispersion tensor D. To do this, the approach used by Tompson et al. (1987) is followed in which a transformation that diagonalizes the dispersion tensor is carried out. By construction, the eigenvectors of the dispersion tensor depend only on the components of the flow velocity but not on the dispersivity values themselves. One eigenvector always points in the direction of the flow velocity. The other two eigenvectors are perpendicular to the direction of flow. The eigenvalue problem for D reads:

$$De_\lambda = \lambda e_\lambda \,, \qquad \text{(Eq. 13)}$$

with eigenvalue λ and eigenvector e_λ. Because the dispersion tensor is symmetric (Bear 1988, p. 611), there exists an orthogonal transformation U that diagonalizes D (Tompson et al. 1987, p. 106, Equation A-3):

$$\tilde{U}DU\tilde{U}e_\lambda = \lambda\tilde{U}e_\lambda, \qquad \text{(Eq. 14)}$$

with

$$\tilde{U}DU = \hat{D}, \qquad \text{(Eq. 15)}$$

where $\hat{D}$ is a diagonal matrix, and U satisfies the relations:

$$U\tilde{U} = \tilde{U}U = I. \qquad \text{(Eq. 16)}$$

Expressing $\hat{D}$ in the form

$$\hat{D} = Q\tilde{Q}, \qquad \text{(Eq. 17)}$$

with Q diagonal, then gives

$$2D = 2U\hat{D}\tilde{U} = 2UQ\tilde{Q}\tilde{U} = 2UQ\tilde{U}\tilde{Q} = B\tilde{B}. \qquad \text{(Eq. 18)}$$

From this relation it follows that the displacement matrix B is given by (Tompson et al. 1987, p. 107, Equation A-10):

$$B = \sqrt{2}UQ. \qquad \text{(Eq. 19)}$$

The implementation of the particle-tracking model requires a finite difference form of Equation 5 at time step n, which in this model is given by

$$X_i^n = X_i^{n-1} + A_i\Delta t + \sqrt{\Delta t}\sum_j B_{ij}Z_j, \qquad \text{(Eq. 20)}$$

with

$$dW_j = Z_j\sqrt{\Delta t}, \qquad \text{(Eq. 21)}$$

for a time step Δt, where Z_j represents a random number. In matrix notation,

$$X^n = X^{n-1} + A\Delta t + \sqrt{\Delta t}BZ. \qquad \text{(Eq. 22)}$$

Sampling Z from a uniform distribution (Tompson et al. 1987, p. 40) leads to the expression:

$$Z = 2\sqrt{3}Z', \qquad \text{(Eq. 23)}$$

with Z' occurring with unit probability over the interval $-\frac{1}{2}$ to $\frac{1}{2}$. Then,

$$< ZZ >= 12 < Z'Z' >= 1, \qquad \text{(Eq. 24)}$$

since

$$< Z'Z' >= \int_{-1/2}^{1/2} Z'^2 dZ' = \frac{1}{12}. \qquad \text{(Eq. 25)}$$

The final step in the derivation is to determine the form of the displacement matrix B. Tompson et al. (1987) derived the expression for an isotropic system, but the equivalent derivation for an anisotropic dispersion model was not available and, hence, is derived below. We assume the anisotropic dispersion tensor is given by Equation 4. The matrix D is symmetric and may be diagonalized as in the isotropic case. Thus, an orthogonal transformation U exists such that

$$\tilde{U}[D - D_0 I]U = \begin{pmatrix} \alpha_L v \\ \alpha_T^H (v_1^2 + v_2^2) + \alpha_T^V v_3^2 \\ \alpha_T^V v \end{pmatrix}. \qquad \text{(Eq. 26)}$$

Thus, in the anisotropic case, the eigenvalues are distinct, and there exist three unique normalized eigenvectors. The matrix U has the form:

$$U = \begin{pmatrix} \frac{v_1}{v} & -\frac{v_2}{\sqrt{v_1^2 + v_2^2}} & -\frac{v_1 v_3}{\sqrt{(v_1^2 + v_2^2)^2 + v_1^2 v_3^2 + v_2^2 v_3^2}} \\ \frac{v_2}{v} & -\frac{v_1}{\sqrt{v_1^2 + v_2^2}} & -\frac{v_2 v_3}{\sqrt{(v_1^2 + v_2^2)^2 + v_1^2 v_3^2 + v_2^2 v_3^2}} \\ \frac{v_3}{v} & 0 & -\frac{v_1^2 + v_2^2}{\sqrt{(v_1^2 + v_2^2)^2 + v_1^2 v_3^2 + v_2^2 v_3^2}} \end{pmatrix}. \qquad \text{(Eq. 27)}$$

The columns of U form an orthonormal set of eigenvectors of D. This transformation, however, becomes singular if $v_1 = v_2 = 0$. In this case, the dispersion tensor is diagonal, and the transformation matrix U is not needed.

The dispersion tensor for an anisotropic system reduces to the isotropic case for equal transverse horizontal and vertical dispersivities. Because the eigenvectors are independent of the dispersivity coefficients and depend only on the flow velocity, the eigenvectors for the anisotropic case must also be eigenvectors for the isotropic case. However, the converse is not true.

For the anisotropic case, the matrix Q is given by

$$Q = \begin{pmatrix} \sqrt{\alpha_L v + D_0} & 0 & 0 \\ 0 & \sqrt{\alpha_T^H \frac{(v_1^2 + v_2^2)}{v} + \alpha_T^V \frac{v_3^2}{v} + D_0} & 0 \\ 0 & 0 & \sqrt{\alpha_T^V v + D_0} \end{pmatrix} \quad \text{(Eq. 28)}$$

The displacement matrix B, thus, has the form:

$$B = \begin{pmatrix} \frac{v_1}{v}\sqrt{2(\alpha_L v + D_0)} & -\frac{v_2}{\sqrt{v_1^2 + v_2^2}}\sqrt{2\left[\frac{\alpha_T^H (v_1^2 + v_2^2) + \alpha_T^V v_3^2}{v} + D_0\right]} & -\frac{v_1 v_3 \sqrt{2(\alpha_T^V v + D_0)}}{\sqrt{(v_1^2 + v_2^2)^2 + v_1^2 v_3^2 + v_2^2 v_3^2}} \\ \frac{v_2}{v}\sqrt{2(\alpha_L v + D_0)} & -\frac{v_1}{\sqrt{v_1^2 + v_2^2}}\sqrt{2\left[\frac{\alpha_T^H (v_1^2 + v_2^2) + \alpha_T^V v_3^2}{v} + D_0\right]} & -\frac{v_2 v_3 \sqrt{2(\alpha_T^V v + D_0)}}{\sqrt{(v_1^2 + v_2^2)^2 + v_1^2 v_3^2 + v_2^2 v_3^2}} \\ \frac{v_3}{v}\sqrt{2(\alpha_L v + D_0)} & 0 & -\frac{(v_1^2 + v_2^2)\sqrt{2(\alpha_T^V v + D_0)}}{\sqrt{(v_1^2 + v_2^2)^2 + v_1^2 v_3^2 + v_2^2 v_3^2}} \end{pmatrix}$$

(Eq. 29)

Again the displacement matrix simplifies for flow along one of the coordinate axes. For $v = v_1$, Equation 29 reduces to:

$$B = \begin{pmatrix} \sqrt{2(\alpha_L v + D_0)} & 0 & 0 \\ 0 & -\sqrt{2(\alpha_T^H v + D_0)} & 0 \\ 0 & 0 & -\sqrt{2(\alpha_T^V v + D_0)} \end{pmatrix}. \quad \text{(Eq. 30)}$$

For $v = v_2$:

$$B = \begin{pmatrix} 0 & -\sqrt{2(\alpha_T^H v + D_0)} & 0 \\ \sqrt{2(\alpha_L v + D_0)} & 0 & 0 \\ 0 & 0 & -\sqrt{2(\alpha_T^V v + D_0)} \end{pmatrix}. \quad \text{(Eq. 31)}$$

For $v = v_3$:

$$B = \begin{pmatrix} 0 & 0 & -\sqrt{2(\alpha_T^V v + D_0)} \\ 0 & -\sqrt{2(\alpha_T^V v + D_0)} & 0 \\ \sqrt{2(\alpha_L v + D_0)} & 0 & 0 \end{pmatrix}. \quad \text{(Eq. 32)}$$

In summary, the particle trajectory is computed by a finite difference technique expressed in Equation 22. The first displacement term of this equation ($A_i \Delta t$) is deterministic, with A defined in Equation 11. This expression captures the movement of particles in the streamlines defined by the flow field. The term $\nabla \cdot D \Delta t$ is required to correctly reproduce the transport equation for cases in which there are gradients in velocity or dispersion coefficient. It reduces to zero for uniform flow fields and constant dispersivity. What is retained in this case is transport along the flow streamline governed by the flow field. The second term in Equation 22 is a stochastic random-walk term to simulate dispersion, with the form of the matrix B derived for an anisotropic dispersion coefficient tensor in Equation 29.

So far, it has been taken for granted that the local velocity vector is known at all locations in space. We now discuss specific implementation issues associated with incorporating this particle-tracking approach using a velocity field determined from a finite-element code. We now discuss these details for the particle-tracking model as implemented in FEHM V2.10 (STN: 10086-2.10-00). Determination of the advection portion of the deterministic term $A_i \Delta t$ requires

that the local velocity be determined. In this version of the code, we restrict the method to orthogonal finite-element grids. This simplification means that the control volume associated with each grid point is a brick-shaped element. Velocity interpolation within a cell is then determined quickly and easily using the velocity interpolation scheme first derived by Pollock (1988). Using that scheme, the code determines, for a given particle at a given location within the cell, the time required to exit the cell and the location where it leaves. If this time is greater than the time step Δt, the particle location within the cell is computed. If the time is less than the time step Δt, the particle is forced to stop at this location and then proceed in another step within the adjoining cell. This process is repeated until the ending time Δt is reached. At the end of this time step, the term $\nabla \cdot D\Delta t$ is used to deterministically move the particle to correct for gradients in the dispersion coefficient. A simple differencing scheme on the finite-element grid is used to compute these terms. Finally, the random-walk term is applied (the final term in Equation 22) using the B matrix derived above (Equation 29).

For this method to work properly, the time step must be selected such that, on average, a particle takes several time steps within each cell. In a system with large variations in pore-water velocity due to permeability and porosity differences from cell to cell, the appropriate time step can vary greatly throughout the domain. In FEHM, this factor is accounted for by dynamically determining the characteristic time step in an approach similar to that developed by Wen and Gomez-Hernandez (1996). In a given cell, the magnitude of the velocity in the cell is used to scale the time step. The time required to traverse the cell completely in each of the three coordinate directions is computed, and the minimum is determined. Then, a user-defined parameter called the Courant factor is multiplied by this minimum time to obtain the time step for the particle within the cell. This approach ensures that several steps are taken by a particle within a cell but minimizes computational time by tailoring the time step to the characteristic velocity within each cell.

Applying the random-walk method on grids and flow fields, such as the saturated-zone flow model, it was found that the theoretically simple inclusion of the $\nabla \cdot D\Delta t$ term to correct for velocity gradients may not be sufficient to account for regions with highly variable velocity fields. In short, computation of $\nabla \cdot D$ on the scale of the finite-element grid may not be sufficient to capture the magnitude of this term adequately. For example, in high-permeability zones immediately adjacent to confining units of low permeability, the gradient is not captured sufficiently accurately to prevent the artificial meandering of a small number of particles into the low-permeability region. As a result, some particles are held up for an unrealistically long time in these zones, resulting in a nonconservative tailing of the solute breakthrough curve at a downstream location. To correct this problem, a user-defined velocity-scaling parameter can be defined to prohibit particles from entering the low-velocity domain by random-walk processes. If the ratio of the velocity before and after the random-walk jump is less than this parameter, the code prohibits the jump, and the particle is returned to the original position where another jump is taken with a different set of random numbers. This simple correction serves the same purpose as the $\nabla \cdot D\Delta t$ term but is more foolproof in maintaining a physically meaningful set of random-walk jumps.

To report the results of a particle-tracking simulation, two options are available. The first requires the definition of a zone consisting of a set of finite-element grid points representing a portion of the model domain where transport results are desired. For example, a "compliance

boundary," which is a given distance from the repository, can be defined by listing all of the nodes in the boundary. Then the code determines the first arrival time of each particle at any node in this fence and reports the cumulative arrival time distribution for all particles. This arrival-time distribution can then be converted to a pumping-well concentration, and the resulting curve can be used as the input to the convolution portion of the PA analysis. Alternatively, the concentration of particles at any cell in the finite-element domain can be reported as the number of particles residing in the cell divided by the fluid mass in the cell. Concentrations computed in this way represent the in-situ concentration in response to the injection of a pulse of solute at time 0. To obtain the cumulative breakthrough curve, we may perform a time integration of these results, yielding the in-situ concentration breakthrough curve at the node in response to a step change in concentration. Both pulse and step response curves can be obtained in the FEHM particle-tracking code.

6.2 MATRIX DIFFUSION

To incorporate the influence of sorption and matrix diffusion, the residence time transfer function (RTTF) particle-tracking method outlined in the FEHM Models and Methods document (Zyvoloski et al. 1997, pp. 41–42) has been adapted to the particle-tracking algorithm. In this method, adjustments to the travel time of a particle are made to account for the influence of physicochemical processes such as sorption and matrix diffusion. During its path along a streamline, the particle travel time is governed by a transfer function describing the probability of the particle spending a given length of time on that portion of its path. For a cumulative probability distribution function of particle residence times, the travel time of a particle along this portion of its path is computed by generating a random number between 0 and 1 and determining the corresponding residence time. On average, if a large number of particles travel through this portion of the model domain, the cumulative residence time distribution of particles will reproduce the shape of the transfer function. The form of the transfer function is derived from an analytical or numerical solution to capture the appropriate processes being considered.

In this particle-tracking algorithm, the schematic model depicted in Figure 1 is used to provide a transfer function for the case of fracture flow and diffusion between equally spaced fractures. In this model:

z is the spatial coordinate along the fracture
t is the time
$2b$ is the fracture aperture
$2B$ is the mean fracture spacing
v is the linear groundwater velocity in the fracture
θ is the porosity of the matrix
R' is the retardation factor in the matrix
R is the retardation factor in the fracture
D' is the matrix effective diffusion coefficient
c is the concentration at z along the fracture
c_0 is the source concentration at $z = z_0$.

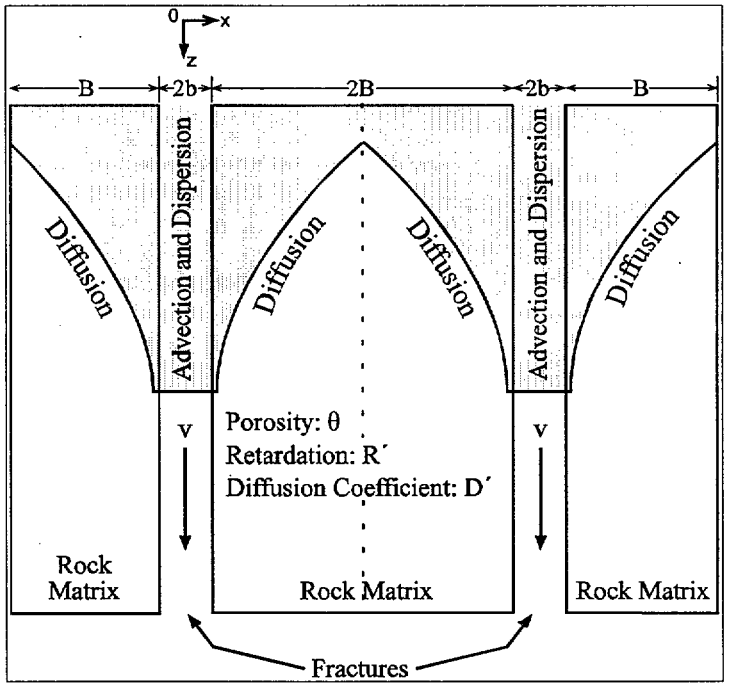

Figure 1. Schematic of the Matrix Diffusion Submodel

The transient solution for contaminant transport with $D = 0$ in parallel fractures, for $c = c_0$ at $z = 0$, and $\partial c/\partial x = 0$ at $x = B$ is given by (Sudicky and Frind 1982):

$$\frac{c}{c_0} = 0, \quad T^0 < 0 \tag{Eq. 33}$$

$$\frac{c}{c_0} = \frac{1}{\pi}\exp\left(\frac{R\lambda z}{v}\right)\int_0^\infty \frac{\varepsilon}{\lambda^2 + \varepsilon^4/4}\exp(\varepsilon_R{}^0)\left[\exp(-\lambda T^0)\left\{\frac{\varepsilon^2}{2}\sin(\varepsilon_I{}^0) - \lambda\cos(\varepsilon_I{}^0)\right\}\right.$$

$$\left. + \frac{\varepsilon^2}{2}\sin(\Omega_I{}^0) + \lambda\cos(\Omega_I{}^0)\right] d\varepsilon, \quad T^0 > 0, \tag{Eq. 34}$$

where λ is a first-order decay constant, ε is an integration variable, and

$$T^0 = t - \frac{Rz}{v} \tag{Eq. 35}$$

$$\varepsilon_R{}^0 = -\frac{\omega\varepsilon}{2}\left(\frac{\sinh(\sigma\varepsilon) - \sin(\sigma\varepsilon)}{\cosh(\sigma\varepsilon) + \cos(\sigma\varepsilon)}\right) \tag{Eq. 36}$$

$$\varepsilon_R{}^0 = -\frac{\omega\varepsilon}{2}\left(\frac{\sinh(\sigma\varepsilon)-\sin(\sigma\varepsilon)}{\cosh(\sigma\varepsilon)+\cos(\sigma\varepsilon)}\right) \quad \text{(Eq. 36)}$$

$$\varepsilon_I{}^0 = \frac{\varepsilon^2 T^0}{2} - \frac{\omega\varepsilon}{2}\left(\frac{\sinh(\sigma\varepsilon)+\sin(\sigma\varepsilon)}{\cosh(\sigma\varepsilon)+\cos(\sigma\varepsilon)}\right) \quad \text{(Eq. 37)}$$

$$\Omega_I{}^0 = \frac{\omega\varepsilon}{2}\left(\frac{\sinh(\sigma\varepsilon)+\sin(\sigma\varepsilon)}{\cosh(\sigma\varepsilon)+\cos(\sigma\varepsilon)}\right), \quad \text{(Eq. 38)}$$

with

$$\omega = \frac{\theta(R' D')^{1/2} z}{bv} \quad \text{(Eq. 39)}$$

$$\sigma = (R'/D')^{1/2}(B-b). \quad \text{(Eq. 40)}$$

Using the transformation variables:

$$\tau_0 = \frac{z}{v} \quad \text{(Eq. 41)}$$

$$\varepsilon_1 = \varepsilon\tau_0^{1/2}, \quad \text{(Eq. 42)}$$

Equations 33 through 42 can be rewritten as:

$$\frac{c}{c_0} = 0, \quad T_1^0 < 0 \quad \text{(Eq. 43)}$$

$$\frac{c}{c_0} = \frac{1}{\pi}\exp(R\lambda\tau_0)\int_0^\infty \frac{\varepsilon_1}{\lambda^2\tau_0^2+\varepsilon_1^4/4}\exp(\varepsilon_R{}^0)\left[\exp(-\lambda\tau_0 T_1^0)\left\{\frac{\varepsilon_1^2}{2}\sin(\varepsilon_I{}^0)-\lambda\tau_0\cos(\varepsilon_I{}^0)\right\}\right.$$

$$\left.+\frac{\varepsilon_1^2}{2}\sin(\Omega_I{}^0)+\lambda\tau_0\cos(\Omega_I{}^0)\right]d\varepsilon_1, \quad T_1^0 > 0, \quad \text{(Eq. 44)}$$

where

$$T_1^0 = \frac{t}{\tau_0} - R \quad \text{(Eq. 45)}$$

$$\varepsilon_R{}^0 = -\frac{\omega_1\varepsilon_1}{2}\left(\frac{\sinh(\sigma_1\varepsilon_1)-\sin(\sigma_1\varepsilon_1)}{\cosh(\sigma_1\varepsilon_1)+\cos(\sigma_1\varepsilon_1)}\right) \quad \text{(Eq. 46)}$$

$$\varepsilon_I{}^0 = \frac{\varepsilon_1^2 T_1^0}{2} - \frac{\omega_1\varepsilon_1}{2}\left(\frac{\sinh(\sigma_1\varepsilon_1)+\sin(\sigma_1\varepsilon_1)}{\cosh(\sigma_1\varepsilon_1)+\cos(\sigma_1\varepsilon_1)}\right) \quad \text{(Eq. 47)}$$

$$\Omega_I^0 = \frac{\omega_1 \varepsilon_1}{2}\left(\frac{\sinh(\sigma_1\varepsilon_1)+\sin(\sigma_1\varepsilon_1)}{\cosh(\sigma_1\varepsilon_1)+\cos(\sigma_1\varepsilon_1)}\right), \quad \text{(Eq. 48)}$$

with

$$\omega_1 = \frac{\theta(R\,D'\,\tau_0)^{1/2}}{b} \quad \text{(Eq. 49)}$$

$$\sigma_1 = \left(\frac{R}{D'\tau_0}\right)^{1/2}(B-b). \quad \text{(Eq. 50)}$$

For the case of no radioactive decay ($\lambda = 0$):

$$\frac{c}{c_0} = \frac{1}{\pi}\int_0^\infty \frac{2}{\varepsilon_1}\exp(\varepsilon_R^0)\left[\sin(\varepsilon_I^0)+\sin(\Omega_I^0)\right]d\varepsilon_1. \quad \text{(Eq. 51)}$$

Therefore, to implement this model, the algorithm requires the input of transport parameters defined in Equations 49 and 50. With the transport parameters and the unretarded travel time τ_0 within a given portion of the path known from the advection part of the particle, values of ω_1 and σ_1 are computed, thereby fully defining the transfer function for this portion of the particle's travel path. Given these parameters, the model returns a value of the delayed travel time of the particle from Equation 45 that is consistent with the matrix diffusion model. To implement this model in FEHM, a series of type curves were generated (CRWMS M&O 2000c) at specified values of ω_1 and σ_1. For given values of the parameters, the code performs a linear interpolation between the nearest type curves to obtain the result. This approach of tabulating the results of the analytical solution is much more computationally efficient than computing the values through integration at run time. Under limiting conditions of low diffusion and/or large fracture spacing, the infinite spacing solution of Tang et al. (1981) implemented in the cell-based particle-tracking algorithm of FEHM can be used instead of the finite spacing model. A provision in the code allows the Tang solution to be invoked in this particle-tracking model as well, but it should be used only when the characteristic diffusion time to the centerline between the fractures (of order B^2/D') is much greater than the time of the simulation.

The final step of the model development is to integrate the matrix diffusion model with the random-walk transport model developed in Section 6.1. Specifically, the time intervals over which the time delays are applied must be set in a manner that allows for computationally efficient and accurate solutions to be obtained. In this model, the time delay is applied to a particle at the time at which it exits a cell, after having determined the cumulative time the particle spent in advective transport through the cell. Within a cell, the transport properties of diffusion and sorption are, by definition, uniform, so that a unique set of transport dimensionless parameters can be defined. Alternatively, the time delay could be applied at each segment of the particle path, resulting in potentially many time delays for a particle within each cell as it is transported by advection and random-walk dispersion. However, in initial prototype testing using this approach, it was determined that the technique, although theoretically equivalent to the application of time delay once per cell, showed that practical limitations of reduced accuracy and

reduced computational efficiency resulted. Therefore, the code was developed with the time delay applied only at the time the particle exits the cell, which can occur either by advection or by random-walk dispersion.

To apply the time delay, the particle is held at that location until the time of the simulation run catches up to the time of that particle, after which the particle is allowed to resume its transport. Finally, it is noted that for sorption without matrix diffusion, the time delay is computed deterministically by computing a retardation factor based on the sorption coefficient K_d, but otherwise, the method is identical to the matrix-diffusion method. Alternatively, this particular case could have been handled through a simple adjustment of the transport velocity, but the implementation using the time-delay method was simpler because it is consistent with the matrix-diffusion method just described.

6.3 TRANSPORT METHODOLOGY VALIDATION

Several test cases have been executed to confirm the accuracy of the particle-tracking method by comparison with analytical solutions. Acceptance criteria will be discussed as each test case is presented. The exact values for the parameters chosen for the test cases are not important because the object of these model runs is to demonstrate the use of the model under conditions similar to those for which the code is intended to be used, namely transport in saturated porous rock under natural or forced gradient flow conditions. All cases reported here are performed on a three-dimensional grid in which flow is aligned with the x-axis. The exact parameterization is unimportant because all that is required of this suite of tests is that the particle-tracking method reproduce the results of an analytical solution carried out at the same flow velocity and dispersion parameters. The grid dimensions are 10 km by 20 km in the horizontal directions and 500 meters (m) thick. In the first test case, the particles are inserted at the inlet within a single cell, and the breakthrough curve at a downstream location (15 km from the inlet) is recorded for the case of longitudinal dispersion with a dispersivity of 100 m. The acceptance criterion for this test case is that a visual comparison ensures that the particle-tracking model is reproducing the analytical solution result to within the resolution of the plot. Figure 2 shows the excellent agreement of the model against the analytical solution. This comparison meets the acceptance criterion. This and the analytical solution results presented in Figures 5 through 7 were generated using the model of Leij et al. (1991), which simulates longitudinal and transverse dispersion in a uniform flow field. This solution is solved using the computer routine 3DADE (see Attachment I). This first test case assumed only longitudinal dispersion. The other test case displayed in the figure illustrates that the particle time-delay method used to simulate a sorbing solute is functioning properly.

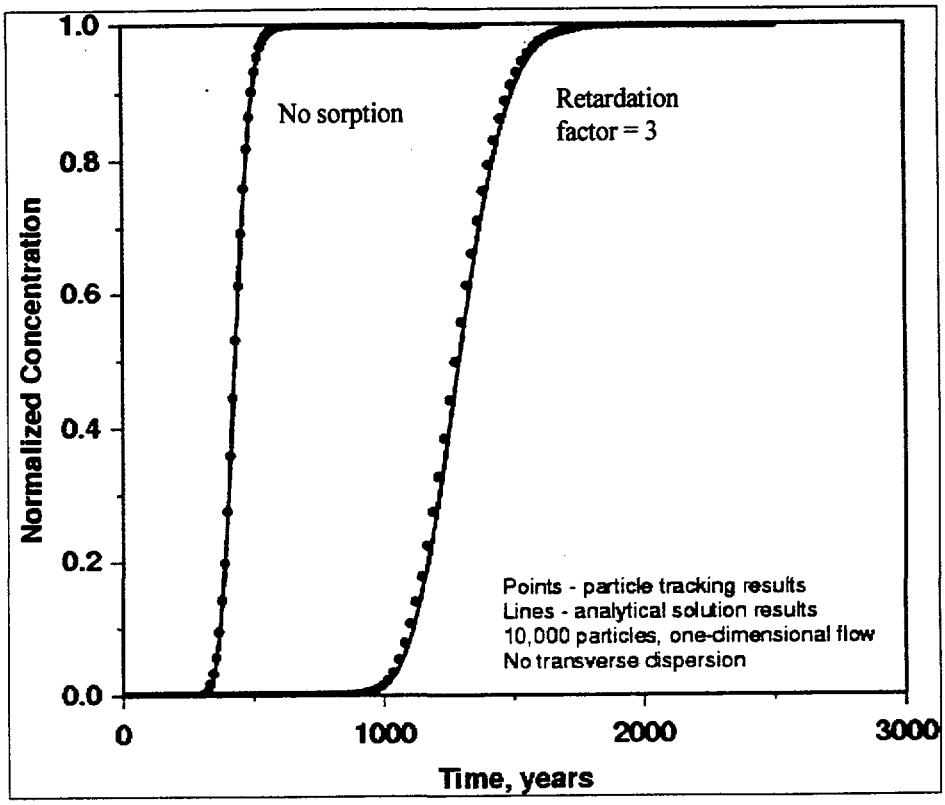

DTN: LA9912BR12213S.001

NOTE: Comparison of breakthrough curves for a conservative and sorbing solute: particle tracking (points) versus analytical solution of Leij et al. (1991) (curves).

Figure 2. Comparison of Particle Tracking and Analytical Solutions

The combination of dispersion and matrix diffusion invokes different portions of the transport model and, thus, must be tested separately. To do this, the same transport problem must first be applied to the case of longitudinal dispersivity of 500 m with matrix diffusion into a semi-infinite matrix. Similar to the previous test case, visual comparison is used as the acceptance criterion. Figure 3 shows that the combined processes of dispersion and diffusion are properly addressed by the algorithm, and that the acceptance criterion is met. For this analytical solution, the option of a semi-infinite matrix derived by Tang et al. (1981) was used to demonstrate the behavior of the model under the limiting conditions of infinite fracture spacing.

Next, the behavior of the particle-tracking code is examined for cases in which the finite fracture spacing solution of Sudicky and Frind (1982) is invoked to demonstrate the behavior of the model when the characteristic distance between flowing fractures is relatively small. In these test cases, dispersion is set to zero to allow for comparison to the analytical solution. For this model, Equation 51 reduces to asymptotic behavior at two limiting extremes of parameters. For very slow matrix diffusion (infinitely small value of the diffusion coefficient), transport times will approach the plug flow travel time within the fractures at the fracture porosity. At the other extreme (large values of the diffusion coefficient and/or small values of the fracture spacing), transport again approaches a plug flow limit, but in this case, the effective porosity is

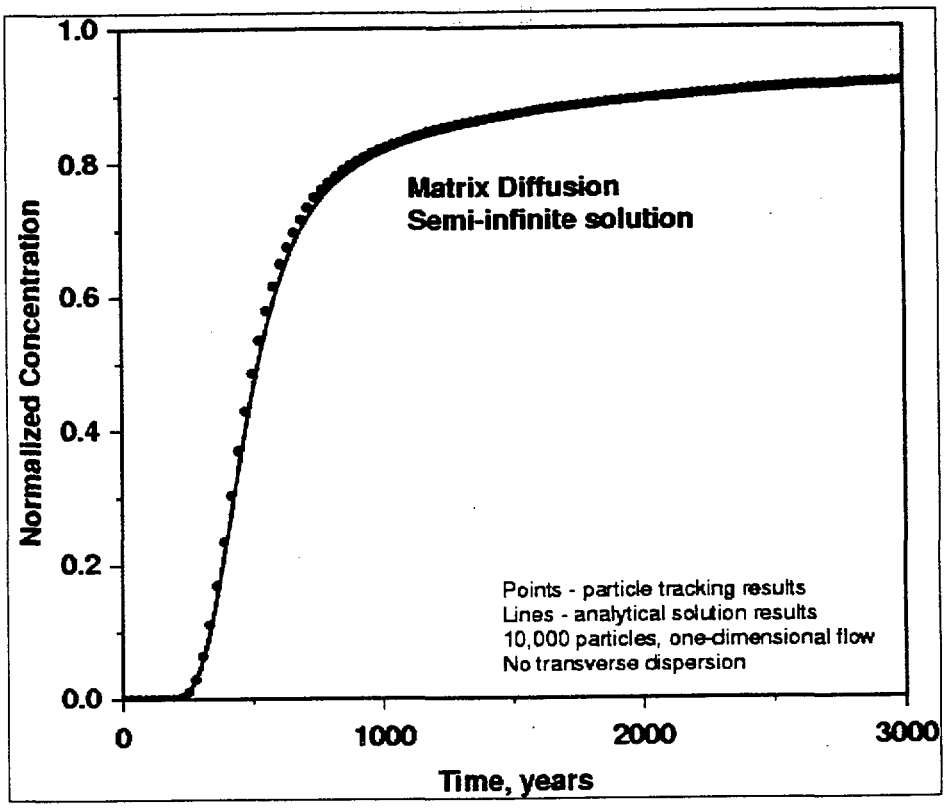

DTN: LA9912BR12213S.001

NOTE: Comparison of breakthrough curves for a solute undergoing longitudinal dispersion and matrix diffusion: particle tracking (points) versus analytical solution of Tang et al. (1981) (curve).

Figure 3. Test of Diffusion and Dispersion

approximately the matrix porosity rather than the fracture porosity. The acceptance criterion for this test case is visual comparison of the particle tracking and analytical solutions, and confirmation that the extremes of possible behavior are not exceeded by the particle-tracking code. Figure 4 shows the results of a series of particle-tracking simulations shown spanning the entire range of transport behavior. The red lines represent the travel times for the limiting cases, with a disparity of more than two orders of magnitude in travel time due to the large difference in porosity (fracture versus matrix). The particle-tracking simulations capture this wide disparity in times. The comparisons of the particle-tracking model and the analytical solution are also shown for small (red curve, short breakthrough time), moderate (the green curves), and large amounts of matrix diffusion (red curve, large breakthrough time). Agreement with the analytical solution meets the visual acceptance criterion, especially considering the wide range of travel time behavior that the code is required to capture.

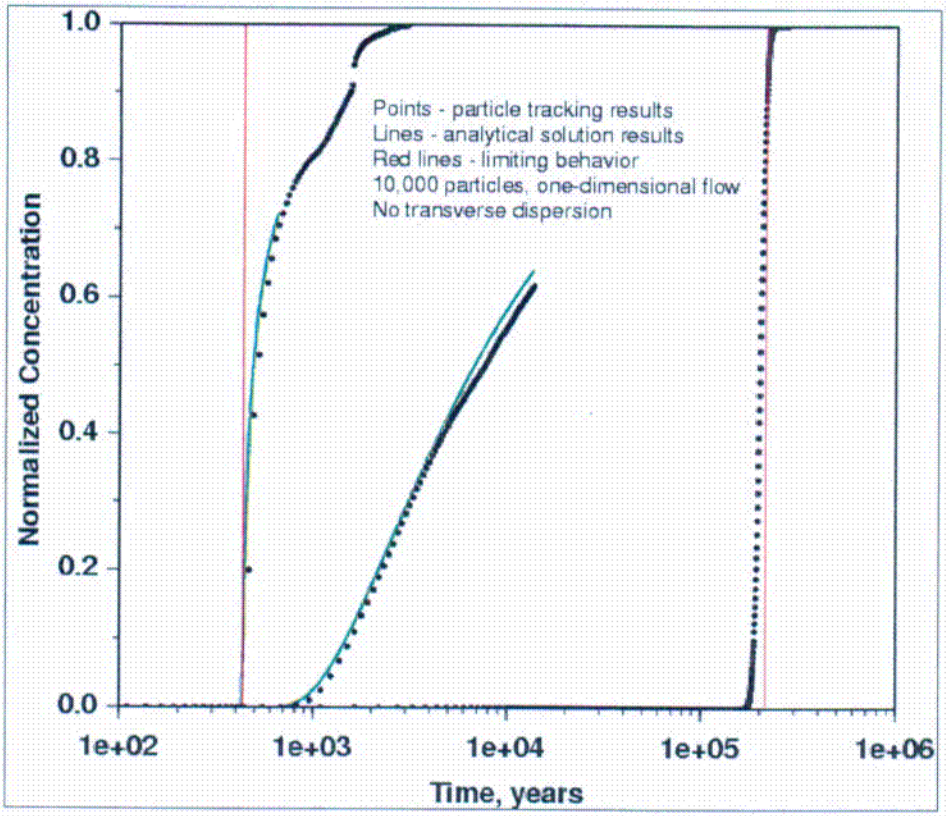

DTN: LA9912BR12213S.001

NOTE: Comparison of breakthrough curves for a diffusing solute: particle tracking (points) versus analytical solution of Sudicky and Frind (1982) (green curves). The red lines are the limiting travel times for no diffusion (short time) and complete diffusion within the matrix (long time).

Figure 4. Test of Diffusion: Sudicky and Frind Model

Up until now, we have only tested cases with (1) diffusion only or with (2) longitudinal dispersion with or without diffusion. The code must also capture the transport behavior for a solute undergoing horizontal and transverse dispersion. A series of simulations were performed with the Sudicky and Frind (1982) analytical solution to validate the ability of the code to capture more complex dispersion cases and to provide accurate in-situ concentrations. For these simulations, the same flow field is used, but the solute is input as a patch on the inlet face of the model. The dimensions of the patch were 3,000 m in the *y*-direction and 12.5 m in the vertical direction, starting at the surface. Particle-tracking model runs, including both longitudinal and transverse dispersion, were carried out with longitudinal dispersivity of 100 m and transverse dispersivity of 0.1 m (values typical of large-scale transport in porous media, after Gelhar 1997). As the plume progresses downstream, spreading in the vertical direction lowers the maximum concentration of particles and allows the particles to migrate to greater depths than the original 12.5 m depth of the plume. At long times, at a constant solute injection concentration, the plume approaches a steady-state concentration distribution within the model. The particle-tracking result is processed by computing the particle plume concentrations for a pulse injection and integrating these results to obtain the constant-injection concentration plume.

C1

As in the previous test cases, the acceptance criterion is visual comparison of the particle tracking results to the analytical solution for the predicted concentration profile. Agreement should become noticeably better when more particles are used, due to the statistical nature of the particle-tracking method. Figure 5 is a plot of concentration versus depth within the plume at various distances from the injection point. For example, the 10,000-m curve is concentration versus depth at steady state at a location 10,000 m downstream from the injection location. The agreement of the particle-tracking model and the analytical solution of Leij et al. (1991) is fairly good (Figure 5), but the particle-tracking result exhibits some noise when only 10,000 particles are injected. Figure 6 is the same simulation for 100,000 particles, illustrating that the particle-tracking model captures the dispersion process more accurately and with less noise when a larger number of particles are used.

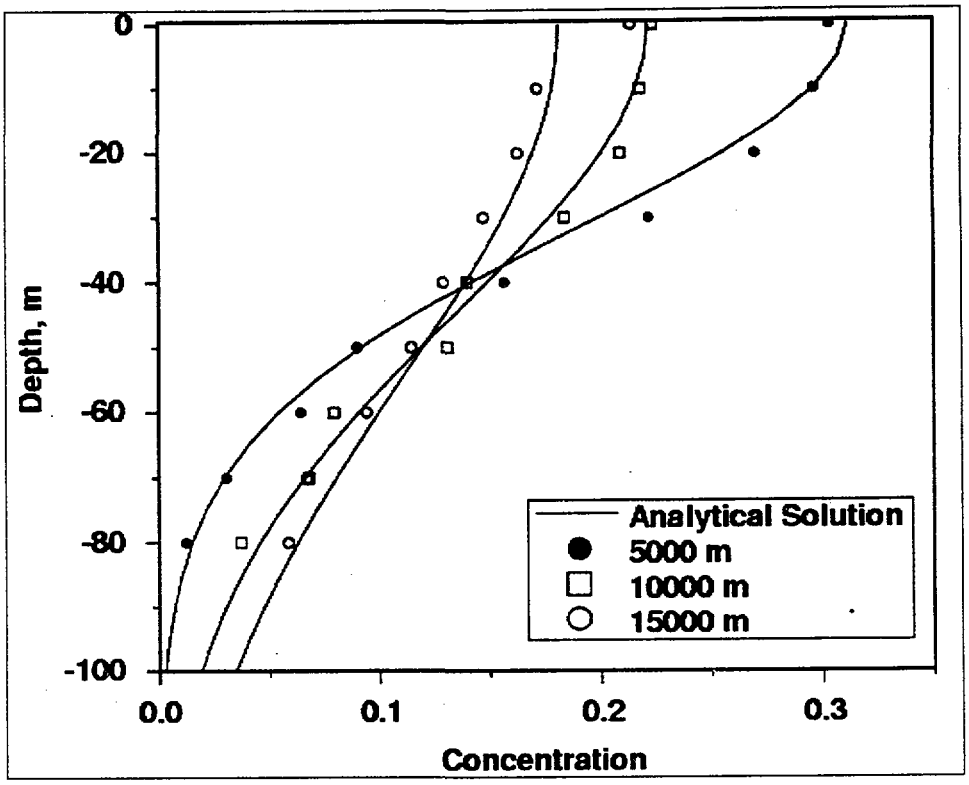

DTN: LA9912BR12213S.001

NOTES: Comparison of steady-state concentration profiles versus depth at various distances along the flow path: particle tracking (points) versus analytical solution of Leij et al. (1991) (curves). 10,000 particles were used in the simulation.

Figure 5. Plume Dispersion Test—10,000 Particles

The final simulation of this set is designed to test the provision to prohibit particles from artificially migrating into low-velocity fluid. In this test case, the model domain is set up with the same permeability in the upper half of the model as in the previous case but with a very low permeability in the bottom half. The same flow velocity is obtained within the high-permeability region, but the velocity is essentially zero in the low-permeability region. Particles are placed in

a patch of the same size as before but immediately adjacent to the low-permeability zone. Particles should travel immediately parallel to the low-permeability zone without migrating into the zone. In fact, the analytical solution is equivalent to that used in Figures 5 and 6, with the depth below the top of the model now replaced by the distance from the low-permeability zone. As in the previous test case, the acceptance criterion is a visual comparison of the particle-tracking model to the analytical solution. Figure 7 shows that the code properly accounts for this behavior, as evidenced by the agreement of the model and the analytical solution. Closer inspection of the results (DTN: LA9912BR12213S.001) reveals that no particles get trapped in the low-permeability zone (all particles reach the outlet of the flow model), which is the desired result.

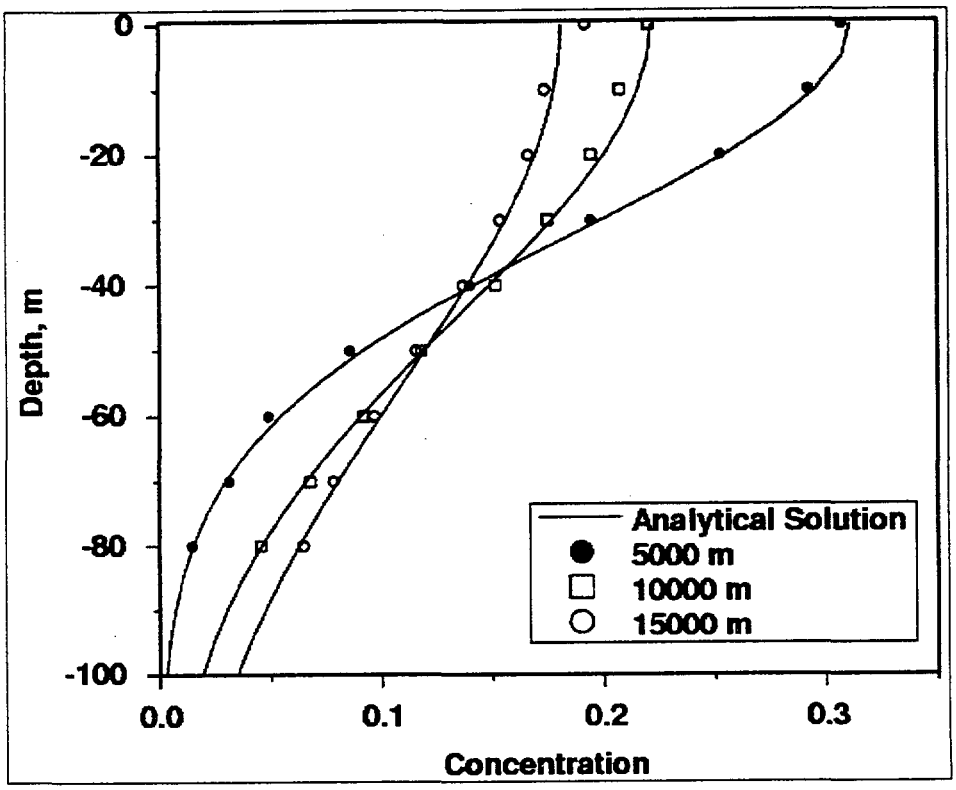

DTN: LA9912BR12213S.001

NOTE: Comparison of steady-state concentration profiles versus depth at various distances along the flow path: particle tracking (points) versus analytical solution of Leij et al. (1991) (curves). 100,000 particles were used in the simulation.

Figure 6. Plume Dispersion Test—100,000 Particles

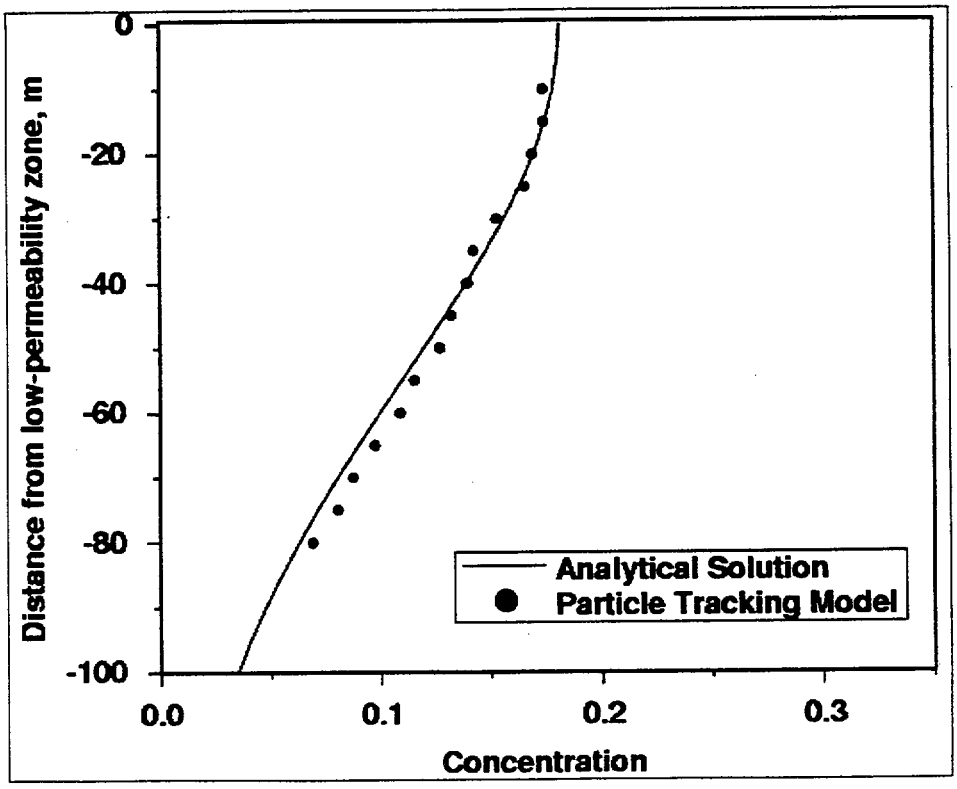

DTN: LA9912BR12213S.001

NOTE: Comparison of steady-state concentration profile versus distance from the low-permeability barrier with distance along flow path = 15,000 m: particle tracking (points) versus analytical solution of Leij et al. (1991) (curves). 100,000 particles were used in the simulation.

Figure 7. Low Permeability Test—100,000 Particles

7. CONCLUSIONS

The particle-tracking algorithm used in this AMR and implemented in FEHM V2.10 (STN: 10086-2.10-00) is suitable for performing saturated-zone flow and transport simulations for the TSPA analyses. The model is a considerable improvement over the TSPA-VA model because it allows transport results to be derived directly from the saturated-zone process model rather than through a cumbersome and difficult-to-justify abstraction process. The flow and transport processes determined to be relevant in the site characterization program are captured with the model. These processes include advection, dispersion, sorption, and matrix diffusion. The capability of assigning a small source region and simulating the transport of a plume that has dimensions that are smaller than the size of a grid block are particularly attractive features of the model. To accomplish these goals, a new form of the particle-tracking formulation needed to be derived to account for anisotropic dispersion—specifically, independent terms for horizontal and vertical transverse dispersivity. In addition, new model development was required to allow for finite spacing between fractures in the matrix-diffusion model. These features were incorporated into FEHM, and extensive validation testing demonstrated that the various processes are adequately captured in the code. Therefore, the particle-tracking model is suitable for use in transport analyses of the saturated zone. However, because FEHM is currently undergoing qualification as per AP-SI.1Q, *Software Management*, quality-affecting output from the code must be given an "unqualified – To Be Verified" status until the software qualification process is complete.

This document may be affected by technical product input information that requires confirmation. Any changes to the document that may occur as a result of completing the confirmation activities will be reflected in subsequent revisions. The status of the input information quality may be confirmed by review of the Document Input Reference System database. Data developed through this AMR may be found as DTN: LA9912BR12213S.001.

INTENTIONALLY LEFT BLANK

8. INPUTS AND REFERENCES

8.1 DOCUMENTS CITED

Bear, J. 1988. *Dynamics of Fluids in Porous Media.* New York, New York: Dover Publications. TIC: 217568.

Burnett, R.D. and Frind, E.O. 1987. "Simulation of Contaminant Transport in Three Dimensions 2. Dimensionality Effects." *Water Resources Research, 23,* (4), 695–705. Washington, D.C.: American Geophysical Union. TIC: 246359.

CRWMS M&O (Civilian Radioactive Waste Management System Management and Operating Contractor). 1998. *Saturated Zone Flow and Transport Expert Elicitation Project.* Deliverable Number SL5X4AM3. Las Vegas, Nevada: CRWMS M&O. ACC: MOL.19980825.0008.

CRWMS M&O 1999a. *SZ Transport Methodology and Transport Component Integration.* Development Plan TDP-NBS-HS-000021 REV 00. Las Vegas, Nevada: CRWMS M&O. ACC: MOL.19990922.0217.

CRWMS M&O 1999b. *M&O Site Investigations.* Activity Evaluation, January 23, 1999. Las Vegas, Nevada: CRWMS M&O. ACC: MOL.19990317.0330.

CRWMS M&O 1999c. *M&O Site Investigations – (Q).* Activity Evaluation, September 28, 1999. Las Vegas, Nevada: CRWMS M&O. ACC: MOL.19990928.0224.

CRWMS M&O 1999d. *Work Package Planning Summary for Saturated Zone Flow and Transport PMR, 1401213SM1, Revision 00.* WPP-NBS-MD-000012. Las Vegas, Nevada: CRWMS M&O. ACC: MOL.19991008.0217.

CRWMS M&O 2000a. *Calibration of the Site-Scale Saturated Zone Flow Model.* MDL-NBS-HS-000011 REV 00. Las Vegas, Nevada: CRWMS M&O. Submit to RPC URN-0191.

CRWMS M&O 2000b. *Modeling Sub Gridblock Scale Dispersion in Three-Dimensional Heterogeneous Fractured Media.* ANL-NBS-HS-000022 REV 00. Las Vegas, Nevada: CRWMS M&O. ACC: MOL.20000622.0363.

CRWMS M&O 2000c. *Type Curve Calculations for Mass Transport in Parallel Fractures Used in Particle-Tracking Scheme in the Saturated Zone.* B00000000-01717-0210-00089 REV 00. Las Vegas, Nevada: CRWMS M&O. ACC: MOL.20000605.0432.

DOE (U.S. Department of Energy) 1998. *Total System Performance Assessment.* Volume 3 of *Viability Assessment of a Repository at Yucca Mountain.* DOE/RW-0508. Washington, D.C.: U.S. Department of Energy, Office of Civilian Radioactive Waste Management. ACC: MOL.19981007.0030.

DOE 2000. *Quality Assurance Requirements and Description.* DOE/RW-0333P, Rev. 10. Washington, DC.: U.S. Department of Energy, Office of Civilian Radioactive Waste Management. ACC: MOL.20000427.0422.

Domenico, P.A. and Schwartz, F.W. 1990. *Physical and Chemical Hydrogeology.* New York, New York: John Wiley & Sons. TIC: 234782.

Dyer, J.R. 1999. "Revised Interim Guidance Pending Issuance of New U.S. Nuclear Regulatory Commission (NRC) Regulations (Revision 01, July 22, 1999), for Yucca Mountain, Nevada." Letter from J.R. Dyer (DOE/YMSCO) to D.R. Wilkins (CRWMS M&O), September 3, 1999, OL&RC:SB-1714, with enclosure, "Interim Guidance Pending Issuance of New NRC Regulations for Yucca Mountain (Revision 01)." ACC: MOL.19990910.0079.

Gardiner, C.W. 1997. *Handbook of Stochastic Methods for Physics, Chemistry and the Natural Sciences.* 2nd Edition. 442. New York, New York: Springer-Verlag. TIC: 247770.

Gelhar, L.W. 1997. "Perspectives on Field-Scale Application of Stochastic Subsurface Hydrology." *Subsurface Flow and Transport: A Stochastic Approach.* Dagan, G. and Neuman, S.P., eds. Pages 157-176. New York, New York: Cambridge University Press. TIC: 247805.

Leij, F.J.; Skaggs, T.H.; and van Genuchten, M.T. 1991. "Analytical Solutions for Solute Transport in Three-Dimensional Semi-Infinite Porous Media." *Water Resources Research, 27,* (10), 2719–2733. Washington, D.C.: American Geophysical Union. TIC: 238367.

Pollock, D.W. 1988. "Semianalytical Computation of Path Lines for Finite-Difference Models." *Ground Water, 26,* (6), 743-750. Worthington, Ohio: National Water Well Association. TIC: 226464.

Reimus, P.W.; Adams, A.; Haga, M.J.; Humphrey, A.; Callahan, T.; Anghel, I.; and Counce, D. 1999. *Results and Interpretation of Hydraulic and Tracer Testing in the Prow Pass Tuff at the C-Holes.* Milestone SP32E7M4. Los Alamos, New Mexico: Los Alamos National Laboratory. TIC: 246377.

Robinson, B.A. 1994. "A Strategy for Validating a Conceptual Model for Radionuclide Migration in the Saturated Zone Beneath Yucca Mountain." *Radioactive Waste Management and Environmental Restoration, 19,* (1-3), 73–96. Yverdon, Switzerland: Harwood Academic Publishers. TIC: 222513.

Sudicky, E.A. and Frind, E.O. 1982. "Contaminant Transport in Fractured Porous Media: Analytical Solutions for a System of Parallel Fractures." *Water Resources Research, 18,* (6), 1634–1642. Washington, D.C.: American Geophysical Union. TIC: 217475.

Tang, D.H.; Frind, E.O.; and Sudicky, E.A. 1981. "Contaminant Transport in Fractured Media: Analytical Solution for a Single Fracture." *Water Resources Research, 17,* (3), 555–564. Washington, D.C.: American Geophysical Union. TIC: 225358.

Tompson, A.F.B. and Gelhar, L.W. 1990. "Numerical Simulation of Solute Transport in Three-Dimensional, Randomly Heterogeneous Porous Media." *Water Resources Research, 26,* (10), 2541–2562. Washington, D.C.: American Geophysical Union. TIC: 224902.

Tompson, A.F.B.; Vomvoris, E.G.; and Gelhar, L.W. 1987. *Numerical Simulation of Solute Transport in Randomly Heterogeneous Porous Media: Motivation, Model Development, and*

Application. UCID 21281. Livermore, California: Lawrence Livermore National Laboratory. ACC: MOL.19950131.0007.

Van Kampen, N.G. 1981. *Stochastic Processes in Physics and Chemistry*. Amsterdam, The Netherlands: North Holland. On Order Library Tracking Number-1745.

Wemheuer, R.F. 1999. "First Issue of FY00 NEPO QAP-2-0 Activity Evaluations." Interoffice correspondence from R.F. Wemheuer (CRWMS M&O) to R.A. Morgan, October 1, 1999. LV.NEPO.RTPS.TAG.10/99-155, with enclosures. ACC: MOL.19991028.0162.

Wen, X.H. and Gomez-Hernandez, J.J. 1996. "The Constant Displacement Scheme for Tracking Particles in Heterogeneous Aquifers." *Ground Water, 34,* (1), 135–142. Worthington, Ohio: National Water Well Journal Publishing. TIC: 246656.

Zyvoloski, G.A.; Robinson, B.A.; Dash, Z.V.; and Trease, L.L. 1997. *Summary of Models and Methods for the FEHM Application—A Finite Element Heat- and Mass-Transfer Code*. LA-13307-MS. Los Alamos, New Mexico: Los Alamos National Laboratory. TIC: 235587.

8.2 CODES, STANDARDS, REGULATIONS, AND PROCEDURES

AP-3.10Q, Rev. 2, ICN 2. *Analysis and Models*. Washington, D.C.: U.S. Department of Energy, Office of Civilian Radioactive Waste Management. ACC: MOL.20000619.0576.

AP-SI.1Q, Rev. 2, ICN 4. *Software Management*. Washington, D.C.: U.S. Department of Energy, Office of Civilian Radioactive Waste Management. ACC: MOL.20000223.0508.

AP-SV.1Q, Rev. 0, ICN 1. *Control of the Electronic Management of Data*. Washington, D.C.: U.S. Department of Energy, Office of Civilian Radioactive Waste Management. ACC: MOL.20000512.0068.

QAP-2-0, Rev 5. *Conduct of Activities*. Las Vegas, Nevada: CRWMS M&O. ACC: MOL.19980826.0209.

8.3 SOFTWARE

LANL 2000. *Software Routine: 3DADE*. Revision 00. MDL-NBS-HS-000010.

Los Alamos National Laboratory 1999. *Software Code: FEHM V2.00*. V2.00. SUN Ultra Sparc. 10031-2.00-00.

Los Alamos National Laboratory 2000. *Software Code: FEHM*. V2.10. SUN Ultra Sparc, PC. 10086-2.10-00.

8.4 OUTPUT DATA, LISTED BY DATA TRACKING NUMBER

LA9912BR12213S.001. Input and Output Files for SZ Transport AMR. Submittal date: 12/23/1999.

ATTACHMENT I:

SOFTWARE ROUTINE 3DADE

Routine: 3DADE Version number: Rev 00

1. SOFTWARE ROUTINE IDENTIFICATION

The 3DADE code was developed under industry standard software Fortran 77. This single-use, software routine is used to verify the particle-tracking methodology described in this AMR.

2. DESCRIPTION AND TESTING

a) Description and Equations of Mathematical Models

This software routine solves the advection-dispersion equation in three dimensions and uses constant concentration (or first-type) boundary conditions at the inlet location of the medium as described by Leij et al (1991, p. 2720)

$$R\frac{\partial C}{\partial t} = D_x \frac{f^2C}{fx^2} - v\frac{fC}{fx} + D_y \frac{f^2C}{fy^2} + D_z \frac{f^2C}{fz^2} - \mu C + \lambda \quad t > 0,\ 0<x<\times,\ -\times <y<\times,\ -\times <z<\times$$

(Eq. I-1)

where

R is the retardation factor
C is the volume averaged or resident concentration of the solute (ML^{-3})
t is the time (T)
x is the position (L) in the direction of flow
y and z are rectangular coordinates, all perpendicular to the flow direction (L)
D_x, D_y, and D_z are dispersion coefficients (L^2t^{-1}) in the x, y, and z directions, respectively
v is the pore-water velocity (LT^{-1})
μ is a general, first-order, rate coefficient for decay (T^{-1})
λ is a general, zero-order, rate coefficient for production ($ML^{-3}T^{-1}$).

The software routine 3DADE has various geometric source-term scenarios for which it solves Equation I-1. This software routine will only encompass one scenario of 3DADE. The general geometry and source location used for the analyses described herein is shown in Figure I-1. This scenario does not account for the rate coefficient for decay or the zero-order rate coefficient for production.

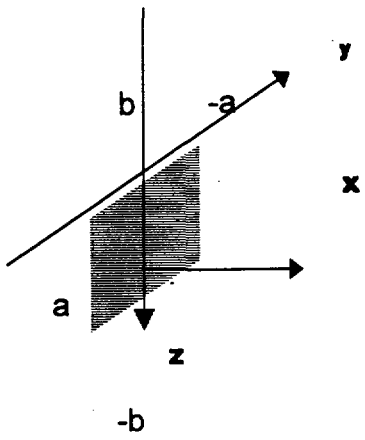

NOTE: The direction of flow is in the *x*-direction, and the water table is located along the *y*-axis. Note that a and –a represent locations along the *y*-axis and b and –b are locations along the *z* axis (the vertical axis).

Figure I-1. Schematic of Inlet and Solute Distribution for a Vertical Rectangular Source in the 3-D Solute Transport Analytical Solution (shown centrally located about the origin of the axes)

b) Description of Software Routine Including the Execution Environment

F. Leij, T. Skaggs, and M. van Genuchten published the theory and applications of 3DADE (Leij et al. 1991). The paper documents the theory, assumptions, and boundary conditions used in deriving the analytical solutions and the corresponding code used to solve the analytical solution.

The executable version of 3DADE was run on the SUN Ultra Sparc workstation at the Los Alamos National Laboratory in Los Alamos, New Mexico. The solution was implemented in FORTRAN and may be complied by any standard FORTRAN 77 compiler.

c) Description of Test Cases

To ensure that the 3-DADE code calculated the analytical solution correctly, a validation problem was designed. The 3DADE analytical solution was verified using a 3-D analytical solution by Domenico and Schwartz (1990, p. 646):

$$C(x,y,z,t) = (\frac{C_0}{8})erfc\left[\frac{(x-vt)}{2\sqrt{\alpha_x vt}}\right]\left\{erf\left[\frac{(y+Y/2)}{2\sqrt{\alpha_y x}}\right] - erf\left[\frac{(y-Y/2)}{2\sqrt{\alpha_y x}}\right]\right\}\left\{erf\left[\frac{(z+Z)}{2\sqrt{\alpha_z x}}\right] - erf\left[\frac{(z-Z)}{2\sqrt{\alpha_z x}}\right]\right\}$$

(Eq. I-2)

where

v is the contaminant velocity
α_x, α_y, and α_z is the longitudinal dispersivity, transverse horizontal dispersivity and transverse vertical dispersivity, respectively
t is time
Y and Z are the source size dimensions
x, y, and z are distances along the respective *x*, *y*, or *z* coordinate axes.

Equation I-2 was used for the test cases to ensure the validity of the 3DADE solution. Two test cases were prepared: Test Case 1 is a breakthrough curve, and Test Case 2 calculates the concentrations as a function of depth. Computer files associated with the test cases below are contained in DTN: LA9912BR12213S.001.

Test Case 1 (Breakthrough Case)

Inputs for the breakthrough case:

Vertical transverse dispersivity = 0.005 m
Horizontal transverse dispersivity = 0.005 m
Longitudinal dispersivity = 50 m
Source size of 3000 m in width and 12.5 m in depth (*z*)
Breakthrough Distance = 20000 m (in the direction of flow)
Retardation = 1.0
Initial concentration = 1.0
Velocity = 100 m/yr.
Time = 2000 yr.
Horizontal distance (*y*) = 0 (perpendicular to the flow direction)
Depth (*z*) = 0 (perpendicular to the flow direction).

The results of the 3DADE code are compared to the solution obtained from Equation I-2 and are shown in Figure I-2.

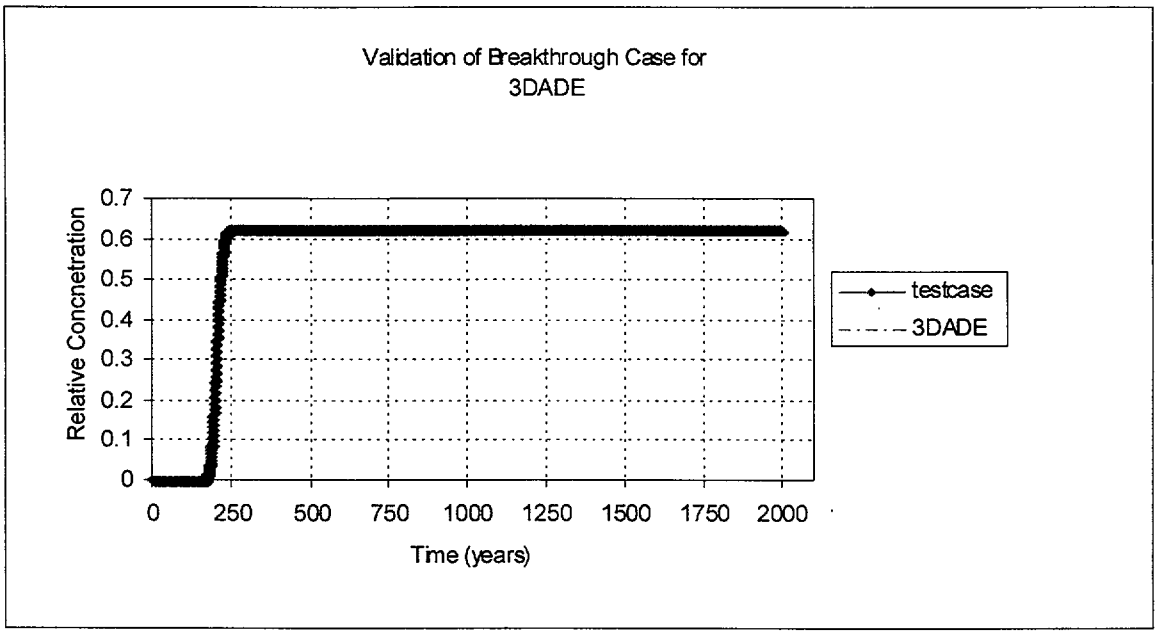

Figure I-2. Breakthrough Test Case Comparing 3DADE and Equation I-2 (labelled "testcase")

Figure I-2 shows that 3DADE and Equation I-2 predict very similar breakthrough curves. The input file for 3DADE is case2_brktr.in.

Test Case 2 (Horizontal Concentrations)

Inputs for Case 2:

Vertical transverse dispersivity = 0.005 m
Horizontal transverse dispersivity = 0.005 m
Longitudinal dispersivity = 50 m
Source size of 3000 m in width and 12.5 m in depth (z)
Breakthrough Distance = 20000 m
Retardation = 1.0
Initial concentration = 1.0
Velocity = 100 m/yr.
Time = 2000 yr.
Horizontal distance (y) = -3000 to 3000 (perpendicular to the flow direction)
Depth (z) = 0 (perpendicular to the flow direction).

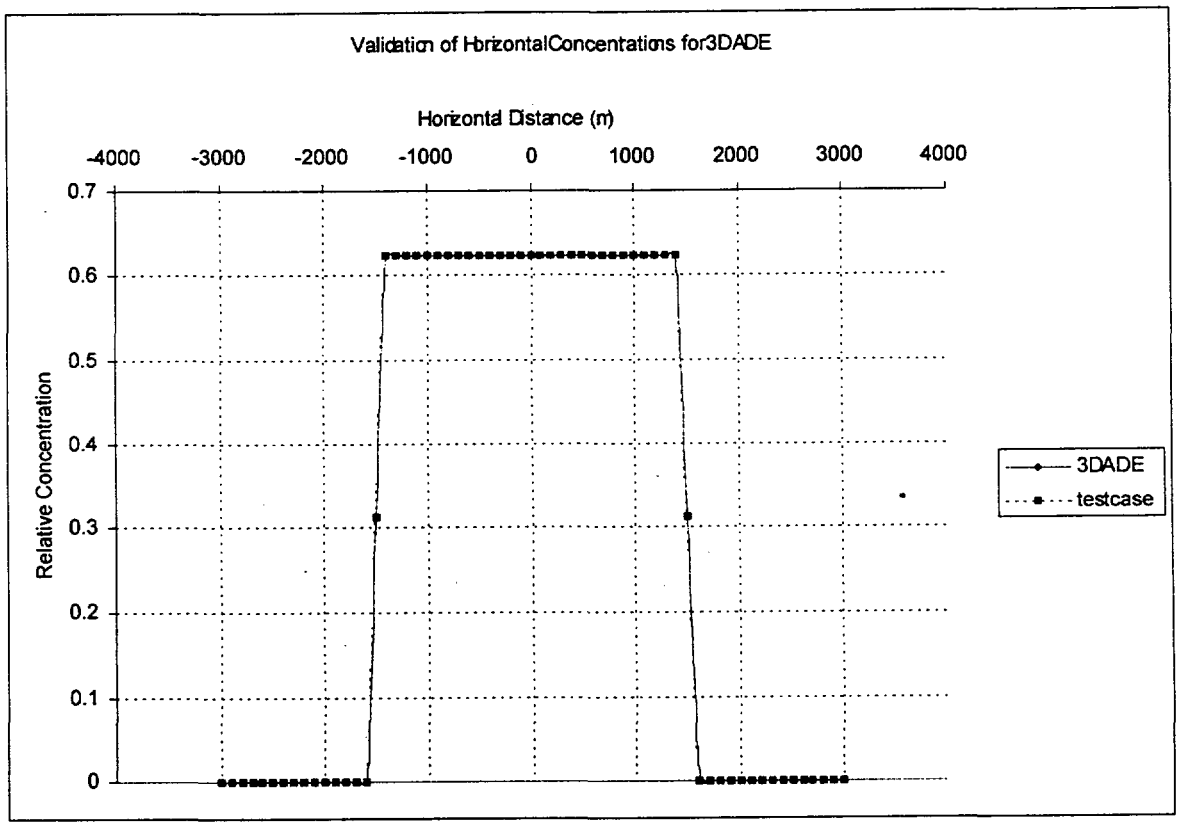

Figure I-3. Comparison of Results from 3DADE and Equation I-2 (labelled "testcase")

Figure I-3 shows that 3DADE and Equation I-2 predict very similar predictions of concentration for horizontal spreading. The input file for 3DADE is case2_horiz.in.

d) Range of Input Parameter Values for which Results were Verified

The 3DADE software routine solves the 3-D advection-dispersion equation and is valid for use in this AMR. Test Cases 1 and 2 are representative samples.

3. SUPPORTING INFORMATION

Electronic file listing:

Software routines

3DADE.for:	Software routine source listing
3DADE:	Executable for 3DADE.for.

Test case files

Validation_brk.xls:

Worksheets:
1) validation_brk: output files from plume software routine and graph of breakthrough test case
2) validation_hor: output file from plume software routine and graph of the horizontal concentrations

***case2_brktr.in:**	Input file for breakthrough curve test case
case2_brktr.out:	Output file for breakthrough curve test case
***plume_casebc.in:**	Input file for horizontal concentration test case
plume_casebc.out:	Output file for horizontal concentration test case.

4. REFERENCES

Domenico, P.A. and Schwartz, F.W. 1990. *Physical and Chemical Hydrogeology.* New York, New York: John Wiley & Sons. TIC: 234782.

Leij, F.J.; Skaggs, T.H.; and van Genuchten, M.T. 1991. "Analytical Solutions for Solute Transport in Three-Dimensional Semi-Infinite Porous Media." *Water Resources Research, 27,* (10), 2719-2733. Washington, D.C.: American Geophysical Union. TIC: 238367.